

Chemical-bath deposition of band-gap-tailored $\text{Cd}_x\text{Pb}_{1-x}\text{S}$ films

H. M. UPADHYAYA, S. CHANDRA*

Department of Physics, Banaras Hindu University, Varanasi, 221 005, India

An attempt was made to modify the band gap of CdS (~ 2.4 eV) by preparing a mixed lattice with a low-band-gap material, PbS (0.3 eV), giving a new set of materials, $\text{Cd}_x\text{Pb}_{1-x}\text{S}$. Band gaps as low as ~ 1.9 eV were achieved with increasing x . The preparation of $\text{Cd}_x\text{Pb}_{1-x}\text{S}$ was carried out by chemical-bath deposition. Structural characterization studies using X-ray diffraction (XRD), energy dispersion analysis by X-rays (EDAX), and optical microscopy were performed. The optical-absorption studies used to find the band gap are also described.

1. Introduction

CdS is one of the most studied materials for solar-cell applications, particularly for photoelectrochemical and heterojunction solar cells. For a photoelectrochemical solar cell (PESC), the ideal band gap of the semiconductor should be ~ 1.6 eV. Unfortunately, the band gap of CdS is high (~ 2.4 eV). We adopted a strategy of preparing solid solutions of a high-band-gap, E_g , material (CdS) with a low-band-gap material (PbS, 0.3 eV), to obtain materials with intermediate band-gap values. The band-gap tailoring of the material $\text{Cd}_x\text{Pb}_{1-x}\text{S}$ with respect to the doping fraction, x , is a consequence of Vegard's law (linear variation of the lattice parameter with the compositions of the two constituents in a solid solution).

The size of the average atom in a solid solution determines the lattice parameter except for miscellaneous binding-energy considerations. Consider a solid solution which is formed between the cubic compounds AC and BC with respective lattice parameters a_{AC} and a_{BC} . If the ratio AC:BC in the solid solution is $(1-x):x$, then the lattice parameter for the solid solution is given by

$$a_{A_{1-x}B_xC} = (1-x)a_{AC} + xa_{BC} \quad (1)$$

This simple linear Vegard's law is generally true in a small compositional range and the above expression may include a parabolic term

$$a_{A_{1-x}B_xC} = (1-x)a_{AC} + x(a_{BC} - a') + a'x^2 \quad (2)$$

The band gap has also been found to vary in a similar fashion to Vegard's law for solid solutions [1–3]

$$\begin{aligned} (E_g)_{A_{1-x}B_xC} &= (1-x)(E_g)_{AC} + x[(E_g)_{BC} - b'] \\ &\quad + b'x^2 \\ &\approx (1-x)(E_g)_{AC} + x(E_g)_{BC} \end{aligned} \quad (3)$$

where a' and b' are the constants controlling the deviation from linearity. The above relation suggests that

band-gap tailoring can be achieved by adjusting the composition of the constituents in a solid solution.

The preparation of CdS (and its solid solutions) can be carried out by a number of processes, including chemical-bath deposition. These processes were extensively surveyed by Stanley [4], Hill [5] and Savelli and Bougnot [6]. Chemical-bath deposition is the simplest of these techniques, in which direct deposition of the material is attained through a chemical reaction in a chemical bath. The chemical-bath technique has an edge over more complicated methods in terms of the relative ease of controlling the parameters, dopants, choice of substrates and in being inexpensive. Kitaev *et al.* [7], Pavaskar and Menzes [8], Chandra and Pandey [9], Mondal *et al.* [10], Danahar *et al.* [11] and Nair and Nair [12] are some of the early workers who used chemical-bath deposition for CdS.

2. Preparation

The experimental arrangement consisted of the following parts which are shown in Fig. 1: (a) a constant-temperature bath ($\sim 80^\circ\text{C}$), (b) a reaction-mixture vessel, (c) a substrate holder with a variable speed motor, and (d) the substrates. The reaction vessel, maintained at 80°C , contained equal volumes of an aqueous one-molar solution of thiourea $\text{CS}(\text{NH}_2)_2$ and CdSO_4 along with different molar concentrations of $\text{Pb}(\text{NO}_3)_2$ to which ammonium hydroxide, NH_4OH (2N), was later added to initiate the reaction. At this stage the well-polished and cleaned substrates were rotated at ~ 125 r.p.m. (revolutions per minute). It was found that films nearly $2\ \mu\text{m}$ thick could be obtained if the time of deposition was kept to about 35 min. Finally, the films were washed with a jet of triply distilled water and then dried and preserved in a desiccator in the dark. All chemicals were AR-grade.

The steps involved in the formation of $\text{Cd}_x\text{Pb}_{1-x}\text{S}$ can be treated on similar lines to the description given

*Author to whom all correspondence should be addressed.

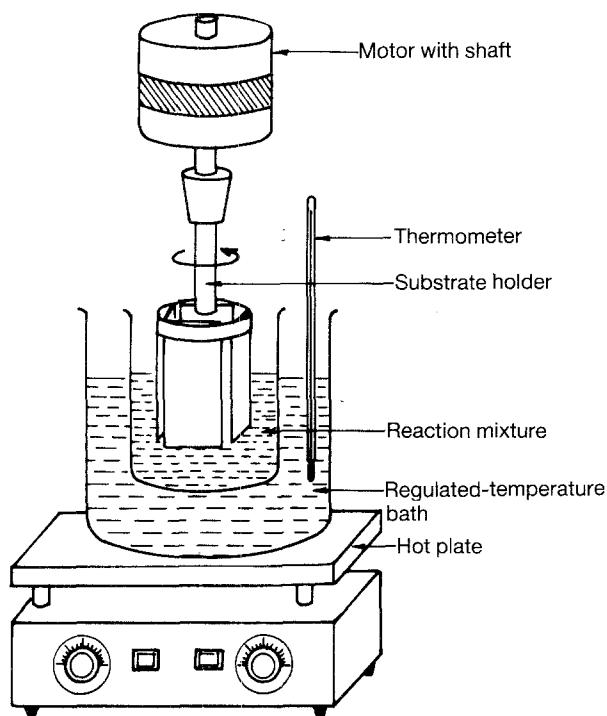
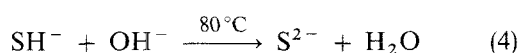
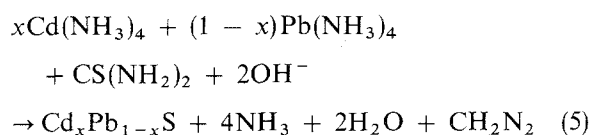


Figure 1 A schematic of the chemical-bath-deposition arrangement for $\text{Cd}_x\text{Pb}_{1-x}\text{S}$ film deposition.

by Pavaskar *et al.* [13] for CdS. Initially, a tetraamine complex of cadmium and lead was formed on addition of NH_4OH , which also supplied OH^- ions. The reaction cell also contained thiourea which released HS^- (thiol group) on dissociation, which combined with hydroxyl ions to form a divalent sulphide ion.



The S^{2-} ions combined with the Cd-and-Pb-tetraamine-complex ions to form $\text{Cd}_x\text{Pb}_{1-x}\text{S}$. The overall reaction giving $\text{Cd}_x\text{Pb}_{1-x}\text{S}$ can be written as



3. Results

3.1. Film morphology and thickness

The thickness of the film was measured with the help of a Surfometer (Model SF-101, Planar Products, UK). The thickness calculated with the help of a surface-profile plot for a $\text{Cd}_x\text{Pb}_{1-x}\text{S}$ ($x = 0.955$) film was $\sim 1.5 \pm 0.3 \mu\text{m}$ (here, the factor $\pm 0.3 \mu\text{m}$ shows the surface roughness of the film).

The surface morphology was studied optically using a Leitz-Metallux 3 optical microscope. The following features were noted.

1. Films of pure CdS were reasonably uniform, except for occasional bright shiny spots which corresponded to the metallic Cd present in the film (Fig. 2a).

2. Excess Cd was present in all the $\text{Cd}_x\text{Pb}_{1-x}\text{S}$ films, and corresponding white shiny spots can be seen in all the micrographs (Fig. 2).

3. In Fig. 2 b, c and d, some black spots corresponding to Pb-nucleation can also be seen in addition to Cd⁻ white spots. These films were obtained with relatively higher concentrations of $\text{Pb}(\text{NO}_3)_2$ as a dopant in the chemical bath (concentration $\geq 0.1 \text{ M}$).

Thus, it is obvious that the segregated Cd and Pb (in highly doped films) are also present in the film separate from the ternary lattice of $\text{Cd}_x\text{Pb}_{1-x}\text{S}$.

3.2. X-ray diffraction studies

X-ray diffraction (XRD) for CdS and various $\text{Cd}_x\text{Pb}_{1-x}\text{S}$ films was performed with the help of a Philips, X-ray diffractometer (model PW 1710). Fig. 3 shows a comparative analysis of all the data. The following conclusions can be drawn.

1. The XRD peaks at low angles ($2\theta = 20-35^\circ$) are superimposed over a broad hump or halo. This is attributed to the partial amorphicity of the films.

2. The films possess mixed structure in the hexagonal and cubic phases identified by the ASTM-X-ray-powder-file data given in Table I.

3. We have taken (1 1 1) at $2\theta = 26.5^\circ$, (2 2 0) at the $2\theta = 43.95^\circ$ and (3 1 1) at $2\theta = 51.95^\circ$ reflections for the cubic phases for calculating the respective lattice parameters. The graded shift of these reflections for XRD of different $\text{Cd}_x\text{Pb}_{1-x}\text{S}$ shows a change in the lattice parameter. This is listed in Table II.

4. The values of x (and hence the stoichiometry of the ternary) was derived using Vegard's law [14]. Fig. 4 shows a theoretical Vegard's plot using a -values for the cubic CdS and PbS of 0.5830 and 0.5938 nm, respectively. From the lattice parameters determined for different $\text{Cd}_x\text{Pb}_{1-x}\text{S}$ films, the values of x , and hence an estimation of the ternary composition of $\text{Cd}_x\text{Pb}_{1-x}\text{S}$, can be read from the theoretical Vegard's plot, as listed in Table III.

5. XRD reflections, corresponding to metallic Cd (in CdS and all $\text{Cd}_x\text{Pb}_{1-x}\text{S}$ films) and metallic Pb (in heavily Pb-doped film compositions of $\text{Cd}_x\text{Pb}_{1-x}\text{S}$) were also observed. This confirms the presence of metallic Cd and Pb which are seen by optical microscopy.

As a consequence of this, we expect that the compositions determined from EDAX shall show a different stoichiometry to that determined by XRD.

3.3. Compositional analysis by EDAX

The determinations of the composition of $\text{Cd}_x\text{Pb}_{1-x}\text{S}$ films were carried out by the energy dispersion analysis by X-rays (EDAX) method. A PV9900 EDAX attachment with a CM-12 (Philips) electron microscope was utilized for the purpose. This instrument allows determination of the stoichiometry of the films using in-built corrections for atomic number, z , absorbance, A , and fluorescence, F , the help of the system software. The following points should be noted.

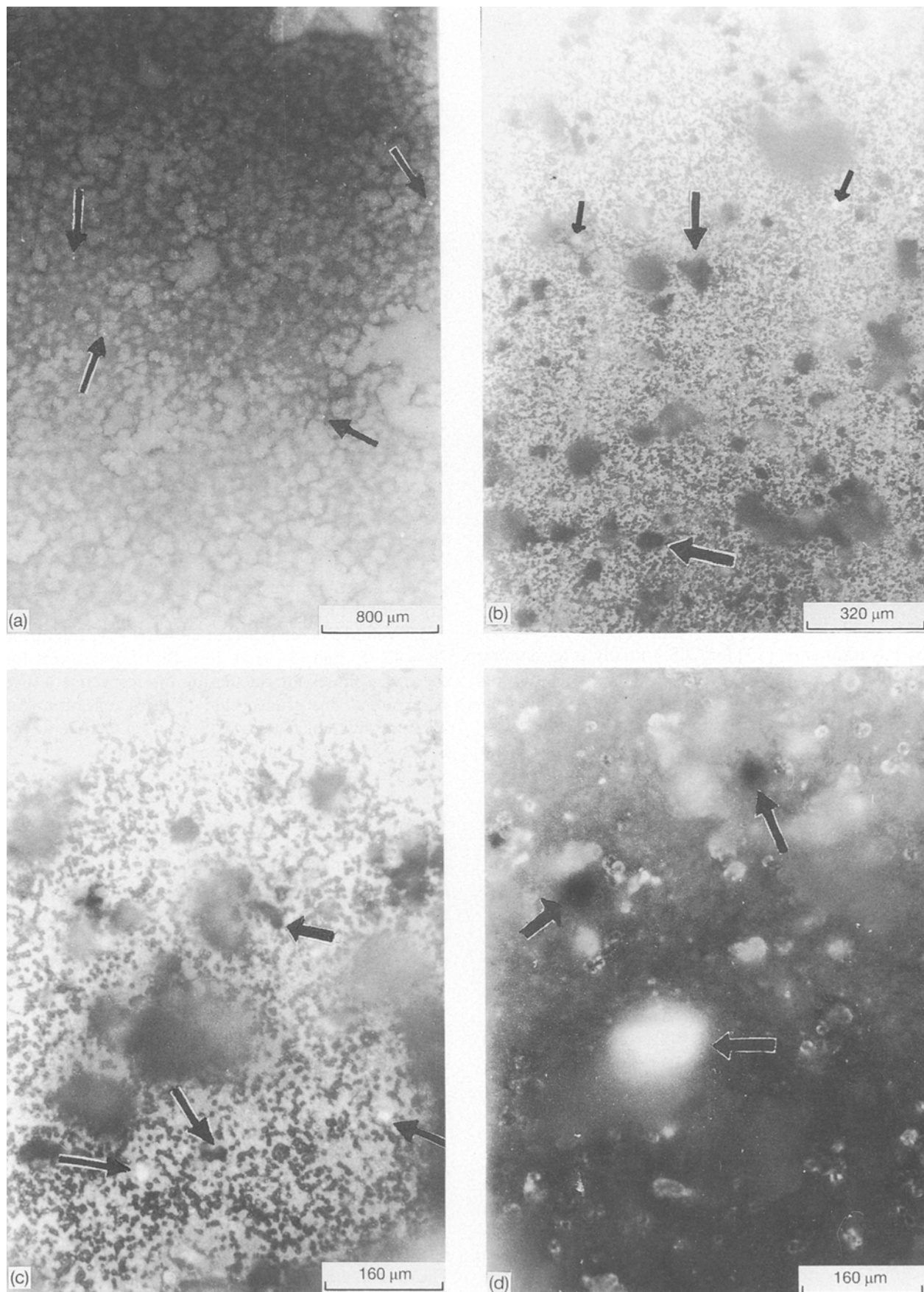


Figure 2 Optical micrographs of different film surfaces with the following compositions: (a) pure CdS, (b) $\text{Cd}_{0.575}\text{Pb}_{0.425}\text{S}$ and (c) and (d) $\text{Cd}_{0.775}\text{Pb}_{0.225}\text{S}$.

1. The conclusion that all films have excess Cd can be drawn after close examination of the EDAX results (see Table III). Table III also gives the compositions of different films, derived from XRD results using

Vegard's approximation. The compositions derived from EDAX do not agree with the compound formula derived from the XRD results. All the films have proportionately more Cd than is required in the ter-

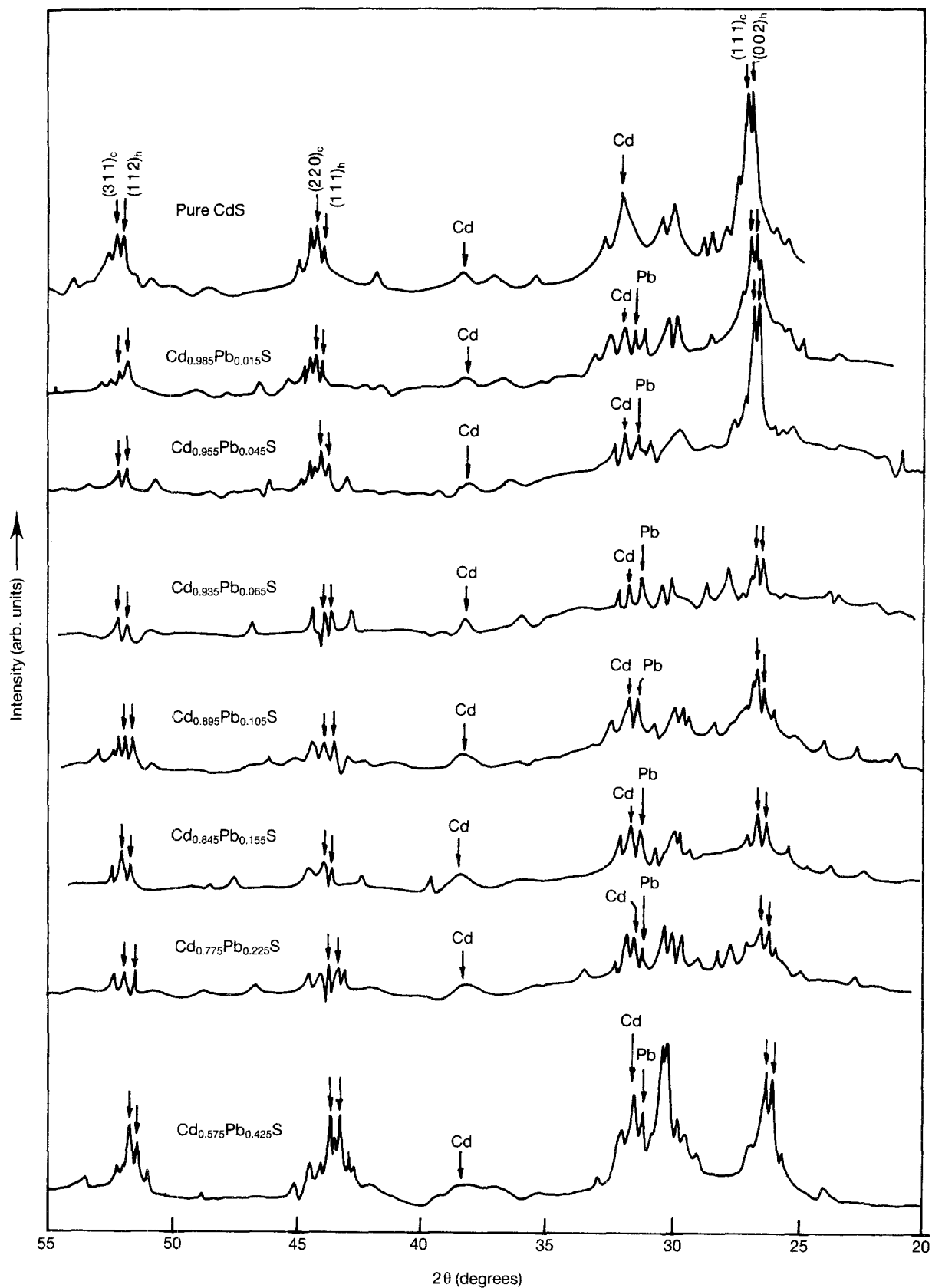


Figure 3 X-ray diffractograms for various $Cd_xPb_{1-x}S$ samples: c, cubic; and h, hexagonal.

nary. While the richness of the atomic percentages of Cd decreases, with decreases in the Pb doping concentrations, it still persists in the pure CdS films.

2. As the $Pb(NO_3)_2$ concentration increases in the chemical bath, more and more Pb enters into the $Cd_xPb_{1-x}S$ composition.

3. For higher Pb doping (≥ 0.1 M $Pb(NO_3)_2$ in the chemical bath), the film showed excess Pb apart from excess Cd. Due to uncertainties in the EDAX, in the XRD and in the theoretical Vegard's law, the presence of excess Pb in low-doped films is not so apparent as the presence of Cd (where the excess is substantial).

TABLE I A comparison of the XRD data with the ASTM-powder-file data for prominent peaks of CdS

Reflections (<i>hkl</i>)	$2\theta_{\text{obs}}$	$(I/I_0)_{\text{obs}}$	d_{obs}	d_{ASTM}	$(I/I_0)_{\text{ASTM}}$	Phase of the crystal
111	26.534	186	3.3592	3.36	100	CdS (cubic)
220	44.042	60	2.0560	2.058	80	CdS (cubic)
112	52.005	62	1.7584	1.761	45	CdS (hexagonal)
101	28.157	61	3.1691	3.16	100	CdS (hexagonal)
002	27.057	88	3.2954	3.36	60	CdS (hexagonal)
002	31.811	106	2.8130	2.81	65	Cd line

TABLE II Lattice constants for cubic lines identified for $\text{Cd}_x\text{Pb}_{1-x}\text{S}$ and CdS using XRD data

Films (the molar concentration of the $\text{Pb}(\text{NO}_3)_2$ used in the bath is given in parentheses)	Identified <i>hkl</i>	$2\theta_{\text{obs}}$	d_{obs} (nm)	Lattice parameters	
				a_{cal} (nm)	a_{cal} (nm) (average)
CdS (pure)	111	26.50	0.3363	0.5826	0.5830
	220	43.95	0.2060	0.5827	
	311	51.95	0.1760	0.5838	
$\text{Cd}_x\text{Pb}_{1-x}\text{S}$ (0.0005)	111	26.45	0.3370	0.5836	0.5832
	220	44.00	0.2057	0.5821	
	311	51.95	0.1760	0.5838	
(0.001)	111	26.45	0.3370	0.5836	0.5835
	220	43.95	0.2060	0.5827	
	311	51.90	0.1762	0.5843	
(0.01)	111	26.45	0.3370	0.5836	0.5837
	220	43.90	0.2062	0.5833	
	311	51.90	0.1762	0.5843	
(0.05)	111	26.45	0.3370	0.5836	0.5842
	220	43.80	0.2067	0.5846	
	311	51.90	0.1762	0.5843	
(0.1)	111	26.40	0.3376	0.5847	0.5847
	220	43.80	0.2067	0.5846	
	311	51.85	0.1763	0.5848	
(0.2)	111	26.35	0.3382	0.5858	0.5854
	220	43.75	0.2069	0.5852	
	311	51.80	0.1765	0.5853	
(1.0)	111	26.25	0.3395	0.5880	0.5875
	220	43.60	0.2076	0.5871	
	311	51.60	0.1771	0.5875	

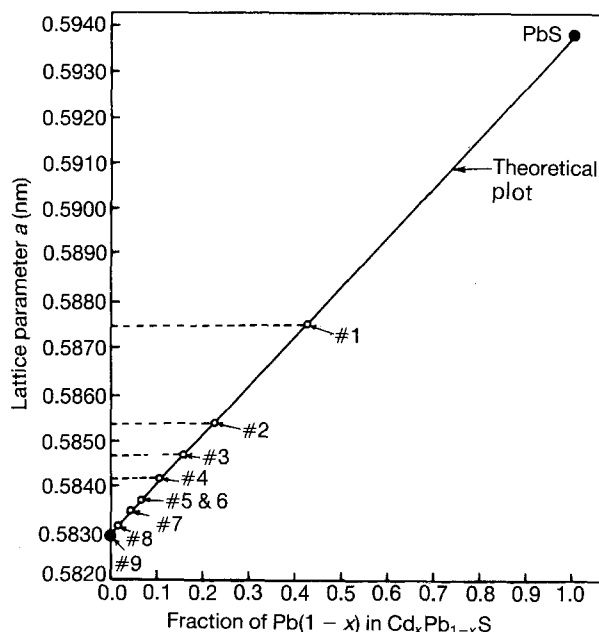


Figure 4 Idealized Vegard's straight-line plot, taking the data of pure CdS and PbS as end reference points. The experimental XRD *a*-values given in Table III were used to derive the stoichiometries of the different films. The derived stoichiometries are: #1 $\text{Cd}_{0.575}\text{Pb}_{0.425}\text{S}$, #2 $\text{Cd}_{0.775}\text{Pb}_{0.225}\text{S}$, #3 $\text{Cd}_{0.845}\text{Pb}_{0.155}\text{S}$, #4 $\text{Cd}_{0.895}\text{Pb}_{0.105}\text{S}$, #5 and #6 $\text{Cd}_{0.935}\text{Pb}_{0.065}\text{S}$, #7 $\text{Cd}_{0.955}\text{Pb}_{0.045}\text{S}$, #8 $\text{Cd}_{0.985}\text{Pb}_{0.015}\text{S}$, and #9 CdS.

TABLE III Composition of $\text{Cd}_x\text{Pb}_{1-x}\text{S}$ films using XRD (Vegard's law) and EDAX data

Film	Composition of alkaline chemical bath (in molarity)		Lattice parameter <i>a</i> (nm)	Bulk composition of the films from EDAX	Estimated ternary composition from Vegard's theoretical plot (XRD data)	Difference in film composition as discussed from EDAX and XRD	
	CdSO_4 + $\text{CS}(\text{NH}_2)_2$	$\text{Pb}(\text{NO}_3)_2$				Excess Cd	Excess Pb
#1	1.0	1.0	0.5875	$\text{Cd}_{2.266}\text{Pb}_{0.716}\text{S}$	$\text{Cd}_{0.575}\text{Pb}_{0.425}\text{S}$	$\text{Cd}_{1.69}$	$\text{Pb}_{0.291}$
#2	1.0	0.2	0.5854	$\text{Cd}_{1.330}\text{Pb}_{0.240}\text{S}$	$\text{Cd}_{0.775}\text{Pb}_{0.225}\text{S}$	$\text{Cd}_{0.555}$	$\text{Pb}_{0.015}$
#3	1.0	0.1	0.5847	$\text{Cd}_{0.990}\text{Pb}_{0.140}\text{S}$	$\text{Cd}_{0.845}\text{Pb}_{0.155}\text{S}$	$\text{Cd}_{0.145}$	—
#4	1.0	0.05	0.5842	$\text{Cd}_{1.123}\text{Pb}_{0.080}\text{S}$	$\text{Cd}_{0.895}\text{Pb}_{0.105}\text{S}$	$\text{Cd}_{0.228}$	—
#5	1.0	0.01	0.5837	$\text{Cd}_{1.050}\text{Pb}_{0.016}\text{S}$	$\text{Cd}_{0.935}\text{Pb}_{0.065}\text{S}$	$\text{Cd}_{0.115}$	—
#6	1.0	0.005	0.5837	$\text{Cd}_{1.240}$	$\text{Cd}_{0.935}\text{Pb}_{0.065}\text{S}$	$\text{Cd}_{0.305}$	—
#7	1.0	0.001	0.5835	—	$\text{Cd}_{0.955}\text{Pb}_{0.045}\text{S}$	—	—
#8	1.0	0.0005	0.5832	—	$\text{Cd}_{0.985}\text{Pb}_{0.015}\text{S}$	—	—
#9	1.0	0.0	0.5830	$\text{Cd}_{1.036}\text{S}$	$\text{Cd}_{1.0}\text{S}_{1.0}$	$\text{Cd}_{0.036}$	—

4. Excess Cd and Pb spots were also seen in the optical micrograph, as discussed previously.

3.4. Optical-absorption studies.

The optical-absorption studies were carried out by using a Hitachi, Model 324 UV/VIS double-beam spectrophotometer. The chemical-bath-deposited films of CdS and $\text{Cd}_x\text{Pb}_{1-x}\text{S}$ were mounted carefully on a fine-quality microscope slide, cut equal to the size of sample holder. A clean glass slide was used as a reference. The absorbance spectra of various compositions of $\text{Cd}_x\text{Pb}_{1-x}\text{S}$ and pure CdS were recorded and compared (see Fig. 5). The most significant observations are as follows.

1. There is a sharp increase in absorbance below a certain wavelength. This sharp increase in absorbance is typical of a direct band-gap semiconductor, a class to which CdS and $\text{Cd}_x\text{Pb}_{1-x}\text{S}$ belong.
2. The band gaps for different $\text{Cd}_x\text{Pb}_{1-x}\text{S}$ films can be calculated using the following relation for the absorption coefficient, α

$$\alpha = \frac{K(h\nu - E_g)^n}{h\nu}$$

where K is a constant, h is the energy of a photon, $n = \frac{1}{2}$ for direct allowed transitions and $n = 2$ for indirect allowed transitions. Since, $\text{Cd}_x\text{Pb}_{1-x}\text{S}$ is a direct band-gap material, the value of n is taken as $\frac{1}{2}$. Consequently, a plot of $(\alpha h\nu)^2$ versus $h\nu$ is expected to be a straight line, as in Fig. 6. The value of E_g here can be calculated from the intercept of these straight line plots. Table IV lists the band gap for various films of $\text{Cd}_x\text{Pb}_{1-x}\text{S}$.

3. The absorbance spectra for high $\text{Pb}(\text{NO}_3)_2$ concentrations (in the chemical bath) viz., 0.2 and 1.0 M show a hump (possibly due to the presence of Pb^{2+}

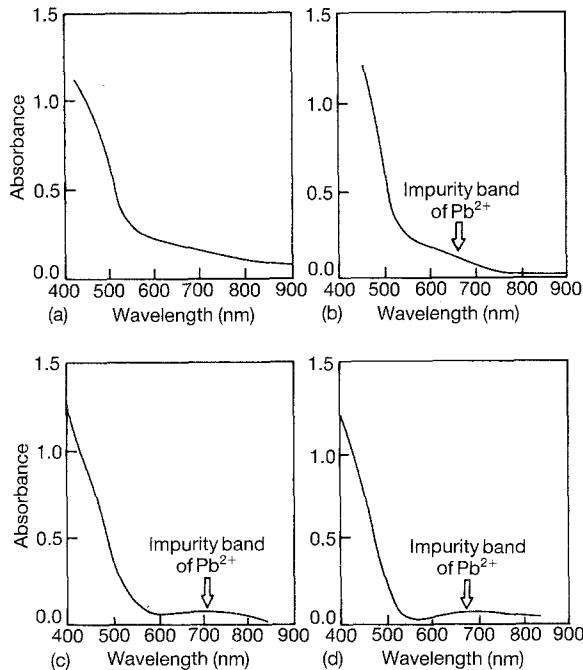


Figure 5 Optical-absorption spectra of films obtained from a chemical bath with the following molar concentrations of $\text{Pb}(\text{NO}_3)_2$: (a) pure CdS, (b) 0.00005 M, (c) 0.2 M, and (d) 0.1 M.

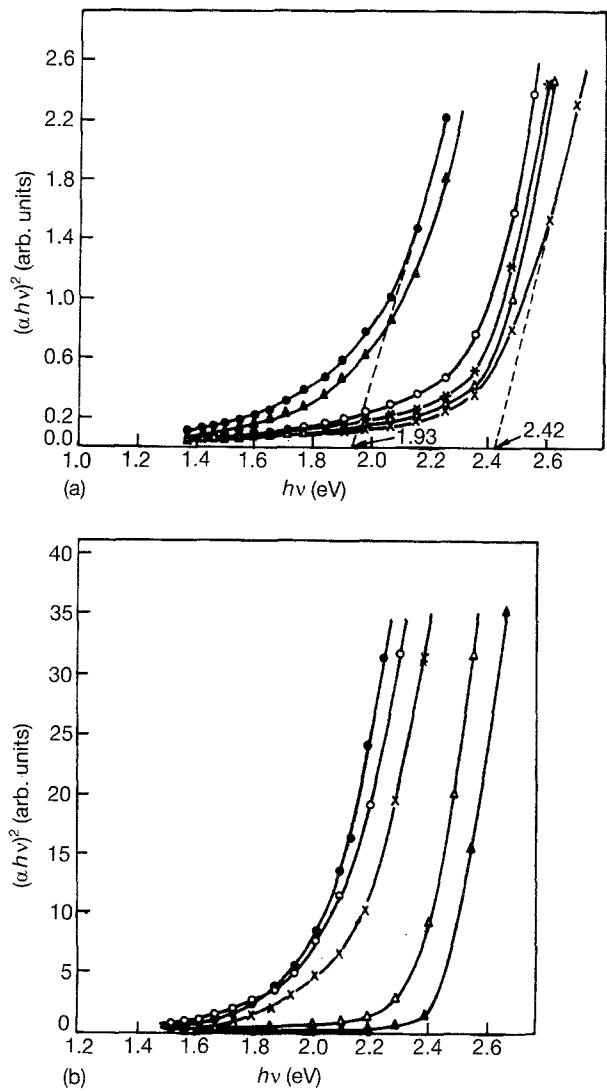


Figure 6 $(\alpha h\nu)^2$ versus $h\nu$ for the determination of the band gap of $\text{Cd}_x\text{Pb}_{1-x}\text{S}$ films: (a) (●) 0.01 M, (▲) 0.005 M, (*) 0.0005 M, (○) 0.0001 M, (△) 0.00005 M, and (×) pure CdS; and (b) 0.05 M, (●) 0.01 M, (×) 0.005 M, (△) 0.001 M, and (▲) pure CdS.

TABLE IV The band gaps of $\text{Cd}_x\text{Pb}_{1-x}\text{S}$ for various molar concentrations of $\text{Pb}(\text{NO}_3)_2$ in the chemical bath

Sample number	Compositions of alkaline chemical bath (molar concentrations)		Composition of the films as obtained from Tables 3 and 4	Band gap (eV)
	$\text{CdSO}_4 + \text{CS}(\text{NH}_2)_2$	$\text{Pb}(\text{NO}_3)_2$		
1	1.0	0.05	$\text{Cd}_{0.895}\text{Pb}_{0.105}\text{S}$	1.94
2	1.0	0.01	$\text{Cd}_{0.935}\text{Pb}_{0.065}\text{S}$	1.92
3	1.0	0.005	$\text{Cd}_{0.935}\text{Pb}_{0.065}\text{S}$	2.14
4	1.0	0.001	$\text{Cd}_{0.955}\text{Pb}_{0.045}\text{S}$	2.31
5	1.0	0.0005	$\text{Cd}_{0.985}\text{Pb}_{0.015}\text{S}$	2.33
6	1.0	0.0001	—	2.29
7	1.0	0.00005	—	2.40
8	1.0	0.00001	—	2.41
9	1.0	0.00	CdS	2.43

excess impurity absorption) just before the absorption edge. Therefore, estimation of the α -value relevant to the application of Equation 3 may lead to erroneous values for determining the value of E_g for such films.

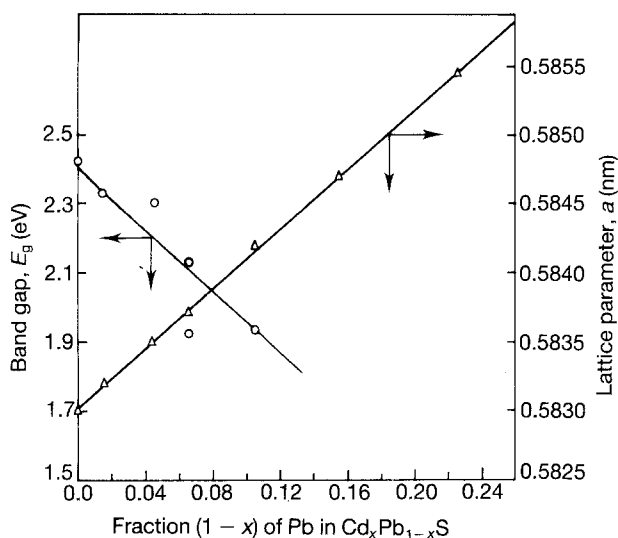


Figure 7 The band gap and lattice constant plotted as functions of the fraction of Pb($1 - x$) for different $Cd_xPb_{1-x}S$ films.

4. Fig. 7 shows a plot between the band gap of different $Cd_xPb_{1-x}S$ compositions, along with the lattice parameter a , versus $1 - x$. The conclusion is obvious: changing the composition results in lattice tailoring which ultimately leads to *band-gap tailoring*.

4. Conclusion

The chemical-bath-deposition technique has been shown to be a successful method for preparing lattice and band-gap tailored $Cd_xPb_{1-x}S$ films with different values of x . The lattice parameter, as well as the band-gap, varies approximately linearly with x . However, we have found that the films obtained by this method are Cd and Pb rich (for high Pb doping).

Acknowledgements

We are grateful to DNES (New Delhi) for the financial support to complete this work. Our thanks are due to Dr O. N. Srivastava, for providing the facilities for XRD and EDAX. We are also grateful to Dr P. C. Mishra for allowing use of the ultraviolet/visible spectrophotometer facility.

References

1. M. A. LITTLEJOHN, T. H. GLISSON and J. R. HAUSER, in "GAIInAsP alloys semiconductors" edited by Pearsall (Wiley, New York, 1982) p. 243.
2. R. E. NAHORY, M. A. POLLACK, W. D. JOHNSTON jr. and R. L. BARNS, *Appl. Phys. Lett.* **33** (1978) 659.
3. B. R. NAG, "Theory of electrical transport in semiconductors" (Pergamon, Oxford, 1972).
4. A. G. STANLEY, in "Applied solid state science", Vol. 5 edited by R. Wolfe (Academic, New York, 1975) p. 251.
5. R. HILL, in "Active and passive thin film devices" edited by J. J. Coutts (Academic Press, New York, 1978).
6. M. SAVELLI and J. BOUGNOT, in "Topics in applied physics, solar energy conversion", Vol. 31 edited by B. O. Seraphin (Springer-Verlag, New York, 1979) p. 213.
7. G. A. KITAEV, A. A. URITSKAYE and S. G. MOKRUSHIN, *Russ. J. Phys. Chem.* **39** (1965) 1101.
8. N. R. PAVASKAR and C. MENZES, *Jpn. J. Appl. Phys.* **7** (1968) 743.
9. S. CHANDRA and R. K. PANDEY, *Phys. Status Solidi (a)* **59** (1980) 787.
10. A. MONDAL, T. K. CHOUDHURI and P. PRAMANIK, *Solar Energy Mater* **7** (1983) 431.
11. W. J. DANAHER, L. E. LYONS and G. C. MORRIS, *ibid.* **12** (1985) 137.
12. P. K. NAIR and M. T. S. NAIR, *ibid.* **15** (1987) 431-440.
13. N. R. PAVASKAR, C. A. MENZES and A. P. B. SINHA, *J. Electrochem. Soc.* **124** (1977) 743.
14. L. VEGARD, *Sko-norske Vidensk. Akad. Mat. Naturv Kbisse* **2** (1947) 83.

Received 10 March
and accepted 8 October 1993